

## PECULIARITIES OF RAMJET COMBUSTION CHAMBER WORK WITH RESONATOR UNDER CONDITION OF VIBRATION FUEL COMBUSTION

A.V. Potapkin, A.A. Pavlov, and D.Yu. Moskvichev

Institute of Theoretical and Applied mechanics SB RAS  
630090 Novosibirsk, Russia

An optical measurement and registration system of electronic radiation of electron-excited radicals OH in flames is presented in this work. To investigate diffusion hydrogen-air torches the mentioned system was used. The obtained experimental data were used for analysis of a thrust formation of the ramjet ejector combustor with acoustic resonator by vibrating burning of hydrogen. It was offered a way to determine geometrical parameters of ejector system and hydrogen consumptions providing the largest thrust values.

Picture registration in different spectral ranges is the central instrument for solution of scientific-technical problems connected with the burning processes. The pictures enable to give a valuable information both about local and integral characteristics of the investigated process. For example, one of the methods of fuel burn-out completeness is based on the effect of OH hydroxide group chemiluminescence which is formed as intermediate product of burning. Act of the OH radical formation is accompanied by a light quantum radiation in the range of 280-350 nm. Intensity of luminous radiation from the controlled flame region in the given spectral range can serve as an index of the reacted fuel quantity.

Figure 1 presents a block-scheme of the registration system for solution of similar problems. The picture of the investigated process 1 with a quartz lens 2 is focused to a photocathode of pin-hole electron-optical converter (EOC) 3. EOC is necessary for transferring a spectral range of registered radiation to a visible range and its enhance. A brightness coefficient can reach 10000 and is adjusted with a power source 4. The image is registered with CCD camera 5. Block of light filters 6 is used for separation of necessary spectral range. To control and account a possible time instability of the tract EOC-CCD-PC a test source of light 7 is used. Control by the test source and the CCD camera is realized with the electron block 8, including an analog-to-digital converter (ADC). Work of the control block is operated by IBM PC 9 that is also used for collection and processing of the obtained information. If necessary, a neutral light filter 10 can be used for decreasing of the image brightness. Operation of the registered system can be synchronized with the investigated processes on the data bus 11. Working spectral range is 0.25-0.7  $\mu\text{m}$ .

Maximum registration frequency of images is determined by a type of the CCD camera, and for the matrix IA-D1-0064 with size 64x64 pixel came to 2000 Hz. Temporal characteristics of the system also depend on quick-action of EOC. At this, time of luminophor afterglow used in an exit screen is a determinative parameter. For the used EOC this value is of  $\tau = 1.5$  ms on level 0.1.

One of the basic parameters of the registered system is a set of transfer functions  $k_{ij}$  which determine a connection between brightness  $I_{ij}$  in every point of initial image on the

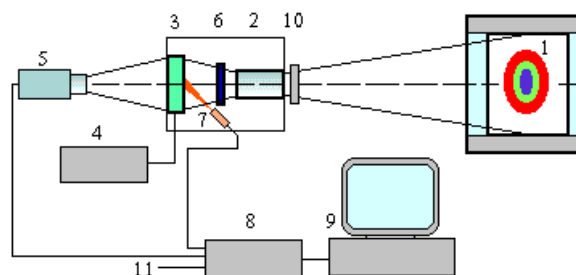


Fig.1. Block scheme of the images registration.

## Report Documentation Page

<b>Report Date</b> 23 Aug 2002	<b>Report Type</b> N/A	<b>Dates Covered (from... to)</b> -
<b>Title and Subtitle</b> Peculiarities of Ramjet Combustion Chamber Work With Resonator Under Condition of Vibration Fuel Combustion		<b>Contract Number</b>
		<b>Grant Number</b>
		<b>Program Element Number</b>
<b>Author(s)</b>		<b>Project Number</b>
		<b>Task Number</b>
		<b>Work Unit Number</b>
<b>Performing Organization Name(s) and Address(es)</b> Institute of Theoretical and Applied Mechanics Institutskaya 4/1 Novosibirsk 530090 Russia		<b>Performing Organization Report Number</b>
<b>Sponsoring/Monitoring Agency Name(s) and Address(es)</b> EOARD PSC 802 Box 14 FPO 09499-0014		<b>Sponsor/Monitor's Acronym(s)</b>
		<b>Sponsor/Monitor's Report Number(s)</b>
<b>Distribution/Availability Statement</b> Approved for public release, distribution unlimited		
<b>Supplementary Notes</b> See also ADM001433, Conference held International Conference on Methods of Aerophysical Research (11th) Held in Novosibirsk, Russia on 1-7 Jul 2002		
<b>Abstract</b>		
<b>Subject Terms</b>		
<b>Report Classification</b> unclassified		<b>Classification of this page</b> unclassified
<b>Classification of Abstract</b> unclassified		<b>Limitation of Abstract</b> UU
<b>Number of Pages</b> 7		

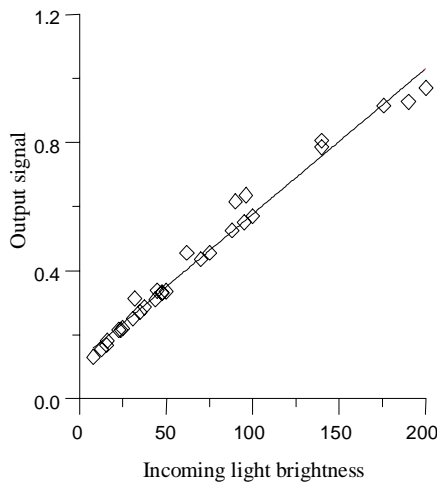


Fig. 2. Output signal for the central part of the image as a function of the incoming light brightness

photocathode of EOC and digital value  $D_{ij}=I_{ij}k_{ij}$  for this point at the system exit. Functions  $k_{ij}$  depend on a power source tension of EOC, a conversion coefficient of ADC, and besides, they can differ for different image points in dependence on constructive peculiarities and quality of the applied EOC. Difference of the EOC amplification factor along the image field is described by so-called zone characteristics, and in this case it accounts not more than 3%.

The most important parameter of the registration system is a conversion coefficient of the initial image brightness to the output digital value which can depend on an input signal value in the whole case. Figure 2 shows a dependence of the output signal for the central region on the source brightness. The obtained dependence is close to the linear one, but there exists a constant component which is due to a slight luminescence of the EOC screen when by input radiation. This demands an appropriate account at the

experimental data being processed. To corroborate the qualitative registration possibilities of radiation intensity and coefficient linearity the systems transmission had been registered and processed taking into account the obtained image dependences of a hydrogen-air torch with equal fuel consumption, but with different input diaphragms. Figure 3 presents the typical torch pictures. A) is an example of the initial pictures, b) are the same pictures transformed taking into account the dependence presented in Fig. 2.

Non-uniformity of transfer characteristics in time can be one from the possible errors at processing of the experimental data. The causes of the similar errors can be the power source instability and consequently, the instability of amplification and transformation factors, a temperature dependence of the electron components parameters, influence of impulse magnetic fields at tube launch, and etc. To consider the similar effects the system was provided with a built test source of light that gave a constant brightness distribution in a non-working image region.

Method of the system calibration depends on a concrete problem and can be realized at the plant directly. This allows to exclude influence of the plant constructive elements, such as absorption and reflection of radiation on the tract optical windows of the wind tunnel, a distance up to the investigated region, observation corners and so on.

Figure 4 shows the typical calibrating curves for completeness of the fuel burn-out on intensity of the OH radical luminescence in the range of the wavelength 0.25-0.35  $\mu\text{m}$ . The dependences of the integral luminescence of the hydrogen torch on the fuel

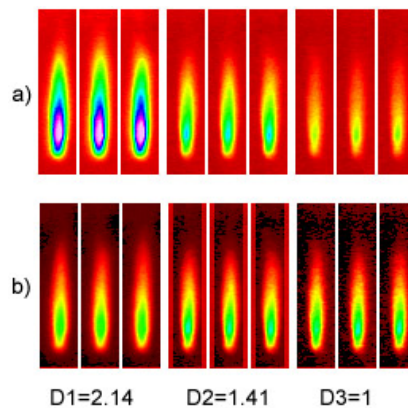


Fig.3. The images of an air-hydrogen flame with different size of relative diaphragm  $D$ . a) – original images; b) – converted images. Flow rate of the fuel is equal to 0.537 litre per second.

consumption are obtained at different sizes of diaphragm of the input D.

It should be noted a sharp incline change of the curve at the fuel consumption 0.2-0.3 l/s. This fact should be accounted very cautiously while determine the consumption completeness on the torch integral brightness at consumptions which are quite different from the consumptions at calibration. The result coincidence for different D confirms once again an efficiency of the registration system and possibility of its application for solution of different problems connected with the combustion processes.

This system was used to obtain the images of the diffusion hydrogen-air torch. Figure 5 presents two types of images obtained by hydrogen burning flowing with supersonic velocity from a nozzle posed horizontally which inner diameter was of  $d = 1.2$  mm by the volume hydrogen consumption  $Q = 2.3$  l/s (for these nozzle sizes the supersonic flow is realized at  $Q > 1.6$  l/s). The image obtained by adjustment of the registration system that allowed to separate torch regions with high radiation intensity, i. e. the burning zones and the high temperature zones of the burning products is presented in Fig. 5, a. At this, in the result of restricted dynamical range (256 brightness gradations) the regions with low brightness intensity had been not registered. It is seen that the flame is separated from the nozzle and a hydrogen jet core is well viewed, besides it is observed a “floating-up” of the burning products because the torch is horizontal. The image of the same torch obtained at a higher system sensitivity is presented in Fig. 5, b. At this, the regions with the high luminescence intensity are not viewed (overfilling of ADC), however, the regions with low luminescence intensity are registered, i. e. the regions of thermoluminescence of the burning products. Figure 5 shows the bending lines: 2 is the bending line of a flame front, 4 is a bound of the jet boundary layer. The following parameters were obtained by processing of these images: an angle between the bending lines and length of the non-darkened zone. Comparison of the images in Fig. 5 and 5, b allows to ascertain a length of the zone with the high radiation intensity (burning zones), and, it is seen that the angle between the bending lines in Fig. 5, b is larger then in Fig. 5, a. Here longitudinal and transverse scales is shown too.

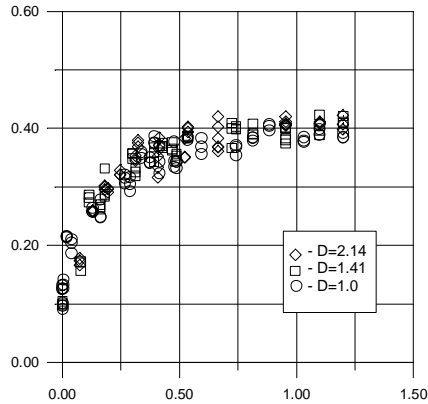


Fig. 4. Integral brightness of the converted images versus the flow rate.

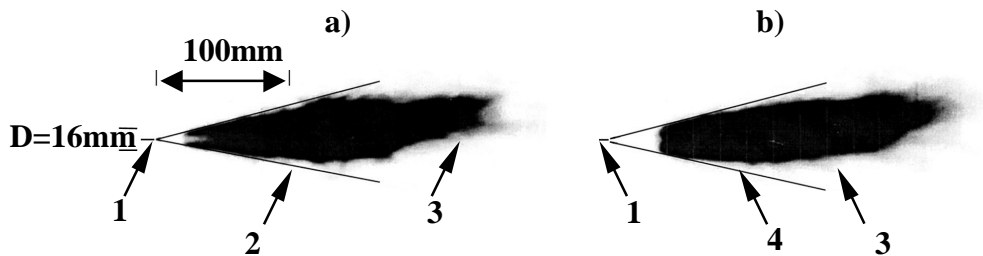


Fig. 5. Image of torch.

a) – large exposition, b) – small exposition.

1 – nozzle, 2 – envelope of flame front, 3 – torch bound, 4 – bound of the jet boundary layer.  $Q = 2.3$  l/s, injector diameter is of 1.2 mm.

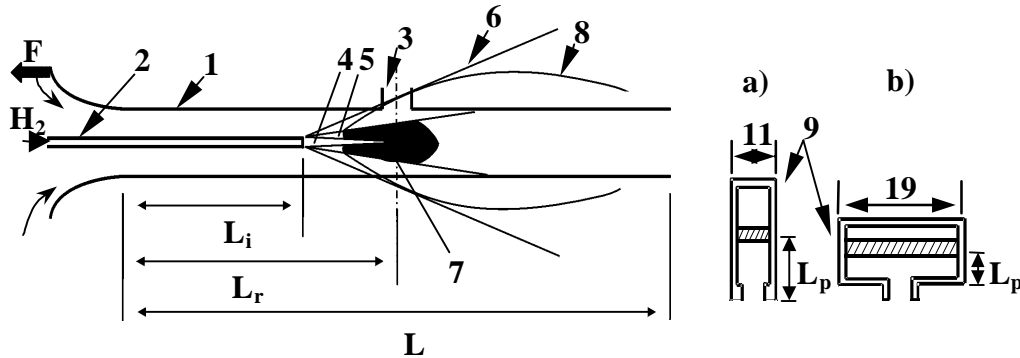


Fig. 6. Scheme.

$L$  is the chamber length,  $L_r$  is position of the resonator,

$L_i$  is position of the injector,  $L_p$  is position of the piston.

1 is a tube, 2 is an injector, 3 is the connection pipe for a resonator, 4 is a jet core, 5 is a region of the flame separation, 6 is a bound of the jet boundary layer, 7 is a combustion region, 8 is a torch bound, 9 are the types of resonators.

Information obtained by the images processing was used for data analysis of the experiments of thrust characteristics of ejector combustion chambers with resonators. Combustor and resonators scheme is shown in Fig. 6. The combustor 1 is a cylindrical tube with inner diameter  $D = 16$  mm (this size is shown in comparison with the torch in Fig. 5). The combustor was provided with a confuser probe in which a lower pressure led to development of a thrust force  $F$ . The combustor was fixed on a strain-gauge balance which were used for the thrust measurement. Combustor length  $L$  in the experiments was of the value from 146 up to 150 mm. Connection pipe 3 with inner diameter of 9.8 mm oriented for resonators 9 attachment in different experiments was posed at different distances  $L_r$  from to the chamber entrance. Two types of resonators used in the experiments are shown in Figs. a) and b): a long cylindrical resonator with inner diameter of 11 mm and cylindrical resonator with inner diameter of 19 mm. Resonator cavity length adjusted by a piston position. Distance from the piston up to the combustor is shown by value  $L_p$ . The images of the combustor and diffusion torch are matched in the scheme. It is shown: 2 is the injector, 4 is the jet core, 5 is a region of the flame separation, 6 is a bound of the jet boundary layer, 7 is the burning region, 8 is the torch bound.

Figure 7 presents one of the oscillograms where recordings of thrust  $F$  and sound vibration amplitude  $A$  before the combustor, and also of hydrogen consumption  $Q$  are shown. The oscillogram was obtained for resonator (see Fig. 6, a)  $L_r/2L = 0.251$  at the relative length of the resonator cavity  $L_p/2L = 0.464$  and relative injector position  $L_i/2L = 0.169$ . This oscillogram shows that with increasing of  $Q$  thrust formation is carried out by a jump with an instant amplitude increase of the sound vibrations that is usually observed at changing of vibrating burning regimes (transfer from the first stage of vibrating burning to the stage of advanced vibrating burning). Further increase of  $Q$  consumption leads to uneven decrease of sound vibrations amplitude and to thrust disappearance.  $A$

Fig. 7. Oscillogram.

regime of the advanced vibrating burning is recommenced by decreasing of the hydrogen consumption. By further decrease of consumption the advanced vibrating burning is transformed into the first stage of the vibrating burning.

During processing of the matched images the following fact was found. The resonator becomes active in the process of the thrust formation if the bound of the boundary layer falls into a resonator throat and extent of the burning zone has a length which provides combustion in the resonator throat. This fact allows to predict a region of parameters in which the highest thrust values are reached, though burning in the diffusion torches and burning in pipes has a principal difference.

Figure 8 presents a dependences of thrust  $F$  (in grams of force) and the sound level  $A$  (in decibel) on hydrogen consumption  $Q$ . Figure 8, a shows the dependences for the resonator with diameter 11 mm, at  $L_r/2L = 0.208$  and  $L_p/2L = 0.368$ . The dependences for the same resonator at  $L_r/2L = 0.251$  are presented in Fig. 8, b, the resonator cavity length did not change. Figure 8, c presents dependences for the resonator with diameter 19 mm,  $L_r/2L = 0.251$  and  $L_p/2L = 0.1575$ , this linear size of the resonator was chosen to obtain the same volume as for the two previous cases. Position of the injector in these experiments was the same –  $L_i/2L = 0.169$ . It is seen from comparison of the results of Figs. 8, a and 8, b that if an injector position is fixed a thrust value is essentially depends on the resonator position. By the same values of the sound vibrations thrust value at  $L_r/2L = 0.208$  is almost 4 times smaller than at  $L_r/2L = 0.251$ . These figures show typical effects of hysteresis described in [1] that can be observed on the oscillogram (see Fig.7). Comparison of Figs. 8, b and 8, c shows that the thrust value depends not only on the resonator position but also on a longitudinal size of the resonator cavity that determines its own frequency. Besides, it is seen that a sound level is determined by a form of the resonator cavity. At conservation of the resonator volume, decrease of the cavity length led to decreasing of the sound level from 130 up to 116 dB, to disappearance of thrust and formation of resistance force. It follows that mass exchange between the resonator cavity and combustor at low frequency is not essential in the thrust formation, but the determining factor of this formation is acoustic interaction of the resonator and the combustor.

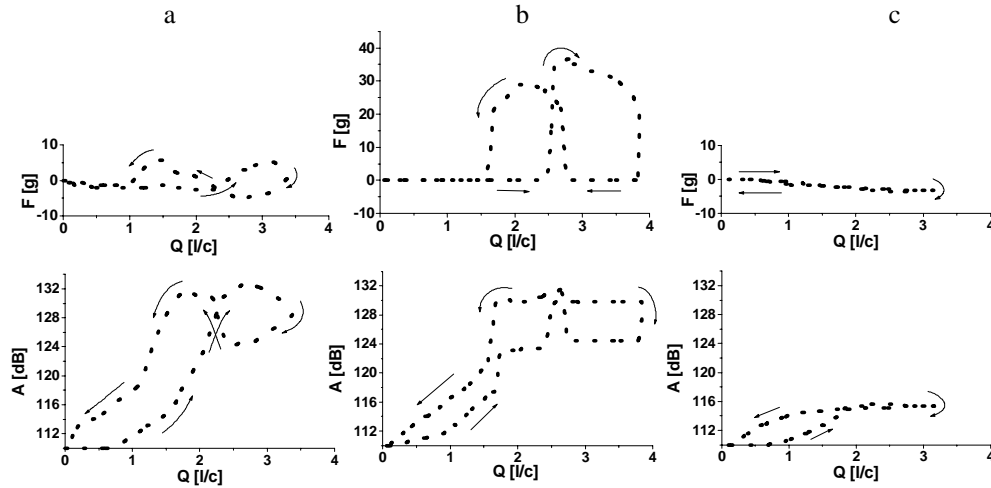


Fig. 8 Thrust and acoustics.

- a)  $L_i/2L = 0.169$ ,  $L_r/2L = 0.208$ ,  $L_p/2L = 0.368$  ( $d = 11\text{mm}$ )
- b)  $L_i/2L = 0.169$ ,  $L_r/2L = 0.251$ ,  $L_p/2L = 0.368$  ( $d = 11\text{mm}$ )
- c)  $L_i/2L = 0.169$ ,  $L_r/2L = 0.251$ ,  $L_p/2L = 0.1575$  ( $d = 19\text{mm}$ )

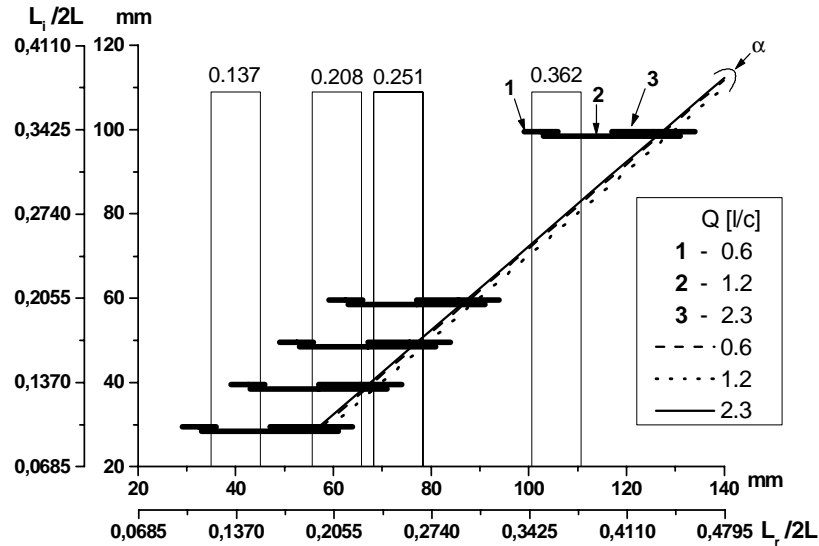


Fig. 9. Summary results.

Figure 9 presents a generalized information about positions of injectors, resonators, on lengths of the burning regions and bound positions of the boundary layers of hydrogen jets. Here, absolute values of the resonator position with inner diameter 11 mm on the combustor and its relative positions  $L_r/2L$  are laid on the abscissa in mm. In figure the resonator diameters are shown by vertical lines above which the relative positions of the resonator throat center are filled on. It is shown four positions of the resonator:  $L_r/2L = 0.137, 0.208, 0.251$  and  $0.362$ . Absolute (in mm) and relative ( $L_r/2L$ ) injector positions in the combustor are laid on the ordinate. Cuts 1, 2 and 3 represent the positions and lengths of the burning regions by hydrogen consumption 0.6, 1.2 and 2.3 l/s accordingly. The crossing points of the boundary layer bound of the hydrogen jet with the combustor walls is shown by lines  $\alpha$  in scheme 6. Analyzing the experimental data it was established that maximum thrust values of the combustor are realized under condition of falling on into the resonator throat the crossing point of lines  $\alpha$  with the cuts which characterizes the burning zones lengths. That, in particular, was illustrated in Fig. 8. It is shown in Fig. 9 that at  $L_r/2L = 0.208$  and  $L_r/2L = 0.133$  the crossing point comes to the trailing edge of the resonator throat. At processing of the results it was found and shown in Fig. 10 that in this point instability of the thrust formation process and the sound level should be expected. Here, a critical value of  $Q$  is value  $\sim 2$  l/s.

On the whole, influence of the resonator on the thrust formation process can be described as follows. At small consumption of hydrogen its burning zone has small sizes, and in the result hydrogen burns so that on the wall chamber and in the resonator throat only burning products are found. By consumption increase the flame is separated from the injector, and on the chamber wall as well as in the resonator throat mixture of hydrogen with air from the jet boundary layer can be found. If length of the resonator cavity is chosen right, the own resonator frequency coincides with one of the own combustor frequencies, and the system “combustor – resonator” operates in the regime of acoustic resonance. With the pressure decrease in the resonator cavity, a mixture of hydrogen with air is soak from the boundary layer in the resonator throat, and right behind from the combustor flame is soak and lights up a fuel mixture in the resonator. By the pressure increase in the resonator, the burning products from the resonator are thrown into the combustor and the flame is thrown off the combustor walls. This

process is repeated cyclically. As it was noted, to realize this process an enough hydrogen  $Q$  consumption should be provided at optimal position of the injector and resonator. A longitudinal resonator size shall correspond to acoustic resonator conditions (in work [2] was obtained multiplicity of the resonator cavity lengths by which maximum values of thrust were reached). It should be noted that for combustors supplied with resonators the maximum thrust values are realized at higher values of the hydrogen consumption than for combustor without resonators. Presence of the resonator leads to actual decrease of the hydrogen volume burned in the chamber at the expense of the resonator volume attached to the chamber. At this, a sound level and thrust increase. Violation of even one from the enumerated conditions lead to the thrust decrease because of decreased energy release. At position of the resonator  $L_r/2L = 0.208$  and position of the injector  $L_i/2L = 0.169$  the hydrogen air mixture does not come into the resonator throat, i. e. a low energy release is taken place, which is seen in Figs. 8, a, 8, b and 9. According to this, the thrust value is occurred 4 times smaller than in case when the resonator is found in position  $L_r/2L = 0.251$ . At the same time, as it was mentioned above, at the resonator position  $L_r/2L = 0.208$  the resonator cavity length is chosen such that it provides an acoustic resonance of the system “combustor-resonator”, that follows from the comparison of the sound levels in Figs. 8, a and 8, b. Violation of other condition – the condition of acoustic resonance of the system (see Figs. 8, b and 8, c) also led to a thrust suppression due to decrease of the sound level and energy release and because of lack of the system acoustic resonance. Possibilities to use the described criteria by the data transfer for diffusion torches in case of vibrating burning in tubes can be evidently justified using the detailed calculations of the flow structure in injector system with burning.

Thus, it is presented an optical system of measurement and registration of luminescence intensity of the electron-excited radicals OH in flames which possesses wide possibilities for study of combustion. This system was used to investigate diffusion hydrogen-air torches. The obtained data were used for analysis of characteristics of the ejector combustor with resonators. The effects of thrust increase was explained and the conditions of realization of the maximum thrust had been formulated.

#### REFERENCES

1. **Potapkin A.V., Moskvichev D.Yu., and Trubitsin A.I.** Hysterises of the acoustic and thrust characteristics of the ramjet combustion chamber at vibration regime of fuel combustion // Intern. Conf. on the Methods of Aerophys. Research: Proc. Pt 1. Novosibirsk, 2000. P. 171-176.
2. **V.K. Baev, D.Yu. Moskvichev, and A.V. Potapkin,** Control by thrust characteristics of ramjet combustion chamber of pulse burning using acoustic resonators // Fizika Gorenia i Vzryva. 2000. Vol. 36, No. 5. P. 3-6.

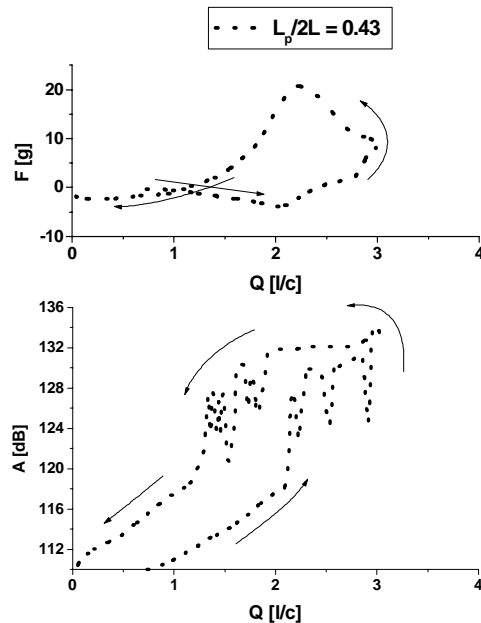


Fig. 10. Instability of the formation process of thrust and acoustics.